Supporting Information

Iron oxide superparamagnetic nanoparticles conjugated with a conformationally blocked α-Tn antigen mimetic for macrophage activation

Massimo Manuelli,[§] Silvia Fallarini,[▽] Grazia Lombardi,[▽] Claudio Sangregorio,[#,§] Cristina Nativi,[§,] Barbara Richichi.*

[§]Dipartimento di Chimica "U. Schiff" and INSTM, Università di Firenze, via della Lastruccia 3, Sesto Fiorentino, I-50019 Firenze, Italy
[#] Istituto di Scienze e Tecnologie Molecolari, Consiglio Nazionale delle Ricerche, via C. Golgi 19, I-20133 Milano, Italy
[▽] Dip. Scienze del Farmaco, Università del Piemonte Orientale Amedeo Avogadro, L.go Donegani 2, I-28100 Novara, Italy

Table of content

Pages

Synthesis of glucosyl derivative for MNPs decoration S3

Synthesis of glucose coated MNPs (GlcMNPs) S6

Synthesis of PEG coated MNPs (PEMNPs) S7

Spectroscopic data and optical rotations S7

Compound 4 S7

Compound 7 S8

Compound 8 S9

Compound 9 S9

Compound 2 S10

Copies of NMR spectra S11

^{1}H (400MHz, $CDCl_3$) Compound 4 S11

^{13}C (100MHz, $CDCl_3$) Compound 4 S12

gDQCOSY (400MHz, $CDCl_3$) Compound 4 S13

gHSQC (400 MHZ, CDCl3) Compound 4 S14

^{1}H (400MHz, $CDCl_3$) Compound 7 S15

^{13}C (50 MHz, $CDCl_3$) Compound 7 S16

gDQCOSY (400MHz, $CDCl_3$) Compound 7 S17

gHSQC (400 MHz, $CDCl_3$) Compound 7 S18

^{1}H (400 MHz, CD_3OD) Compound 2 S19

^{13}C (50 MHz, CD_3OD) Compound 2 S20

gDQCOSY (400 MHZ, CD_3OD) Compound 2 S21

^{31}P (200 MHZ, CD_3OD) Compound 2 S22

Figure S1: TEM image of MNP seeds S23

Figure S2: XRD patterns of MNPs S24

Figure S3: AC susceptibilities and Arrhenius plot S25

Figure S4: DLS of GMNPs S26

Figure S5: TEM images of CMNPs and GMNPs S27

Figure S6: FT-IR spectra of MNPs S28

Figure S7: Effects of 2, CMNPs and GMNPs on cell viability S29

Figure S8: Concentration-dependence of 2, CMNPs and GMNPs uptake S30

Table S1: PCR primers and protocols S31

References S31

Synthesis of glucosyl derivative for MNPs decoration

Synthesis of compound 12

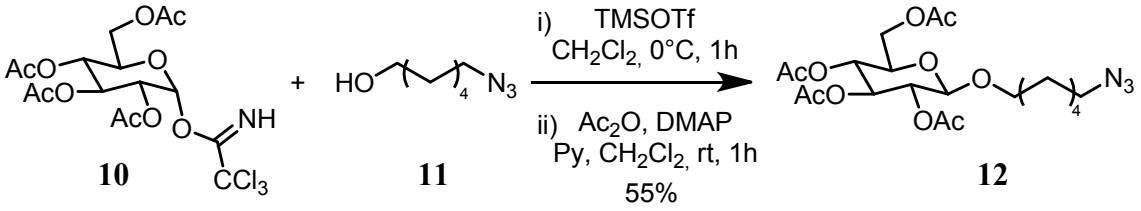

To an ice-cooled solution of **10**[S1] (1.173 g, 2.38 mmol) and **11**[S2] (0.452 g, 3.16 mmol) in CH_2Cl_2 (12 mL) trimethylsilyl trifluoromethanesulfonate (90 µL, 0.5 mmol) was added dropwise. The reaction mixture was stirred at 0°C for 1h, then neutralized with triethylamine (100 µL, 0.72 mmol), diluted with CH_2Cl_2 (230 mL) and washed with a saturated solution of NH_4Cl (2 x 10 mL) and brine (1 x 20 mL). The organic phase was dried over Na_2SO_4 filtered and concentrated to dryness. The crude product (1.55 g) was dissolved in CH_2Cl_2 (10 mL) and then DMAP (0.24 mmol, 30 mg), acetic anhydride (1.13 mL, 11.9 mmol) and pyridine (1 mL, 11.9 mmol) were added. The reaction mixture was stirred at rt for 1h, then diluted with CH_2Cl_2 (220 mL) and washed with a saturated solution of NH_4Cl (3 x 15 mL). The organic phase was dried over Na_2SO_4 filtered and concentrated to dryness. The crude was purified by flash column chromatography on silica gel (petroleum ether/ethyl acetate 3:1) to afford **12** (615 mg, 55% yield) as a white sticky solid. $[\alpha]_D^{25}$ = - 11.7 (c 0.31, $CHCl_3$); ^{1}H NMR (200 MHz, $CDCl_3$) δ: 5.24-4.93 (m, 3H), 4.48 (d, J = 8.0 Hz, 1H), 4.30-4.22 (A part of an ABX system, $J_{A,B}$ = 12.3 Hz, $J_{A,X}$ = 4.6 Hz, 1H), 4.16-4.08 (B part of an ABX system, $J_{B,A}$ = 12.3 Hz, $J_{B,X}$ = 2.6 Hz, 1H), 3.92-3.81 (m, 1H), 3.72-3.63 (m, 1H), 3.52-3.41 (m, 1H), 3.25 (t, J = 6.7 Hz, 2H), 2.07-1.99 (m, 12H), 1.64-1.51 (m, 4H), 1.39-1.31 (m, 4H). ^{13}C NMR (50 MHz, $CDCl_3$) δ: 170.7, 170.4, 169.5,

169.3, 100.9, 73.0, 71.9, 71.5, 70.0, 68.6, 62.1, 51.4, 29.3, 28.9, 26.5, 25.5, 20.8, 20.7. Elemental analysis for $C_{20}H_{31}N_3O_{10}$: calc. C 50.73, H 6.60, N 8.87; found C 50.14, H 6.80, N 9.09.

Synthesis of compound 13

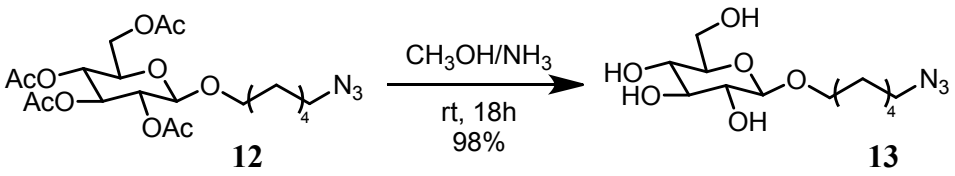

12 **13**

To a solution of **12** (0.579 g, 1.22 mmol) in CH_3OH (2.5 mL), 10 mL of an ammonia solution in methanol (2M) was added. The reaction mixture was stirred at rt overnight and then concentrated to dryness. The crude was filtered on a pad of silica gel (eluent: ethyl acetate) to give compound **13** (0.365 g, 98% yield) as a colorless sticky solid. $[\alpha]_D^{25}$ = - 31.2 (c 0.9, $CHCl_3$); ^{1}H NMR (200 MHz, $CDCl_3$) δ: 5.89 (bs, 1H), 5.42 (bs, 1H), 5.15(bs, 1H), 4.67 (bs, 1H), 4.30 (d, *J* = 7.5 Hz, 1H), 3.92-3.78 (m, 3H), 3.65-3.47 (m, 3H), 3.39-3.24 (m, 4H), 1.73-1.53 (m, 4H), 1.46-1.36 (m, 4H). ^{13}C NMR (50 MHz, $CDCl_3$) δ: 102.9, 75.7, 73.5, 70.3, 69.5, 61.4, 51.4, 29.5, 28.8, 26.6, 25.5. Elemental Analysis for $C_{12}H_{23}N_3O_6$: C 47.20, H 7.59, N 13.76; found C 47.32, H 7.89, N 13.76.

Synthesis of compound 14

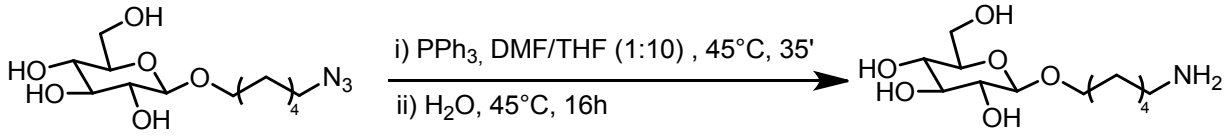

13 **14**

To a stirred solution of **13** (0.083 g, 0.27 mmol) in a mixture DMF:THF (1:10, 5.5 mL) triphenylphosphine (0.147 g, 0.56 mmol) was added. The reaction mixture was stirred at 45°C for 35', then cooled to room temperature and H_2O (40 µL, 2.22 mmol) was added. The solution

was stirred at 45°C overnight the concentrated to dryness. The crude product **14** was used for the following reaction without any further purification.

Synthesis of compound 16

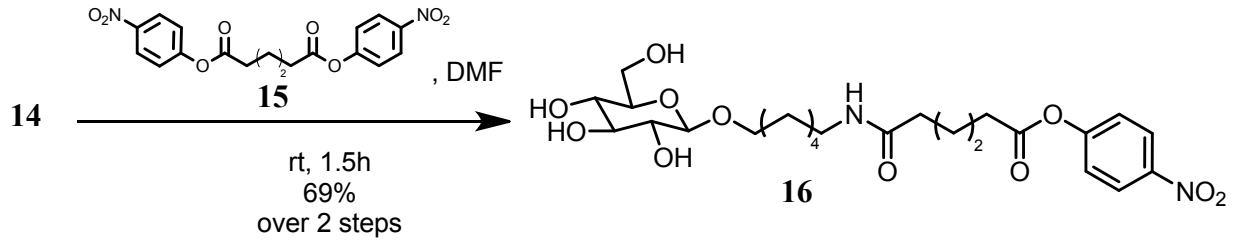

To a stirred solution of crude **14** (0.240 g) in DMF (0.4 mL), a solution of **15**[S3] (0.423 g, 1.09 mmol) in DMF (2.25 mL) was added dropwise. The reaction mixture was stirred at rt for 1.5 h then concentrated to dryness. The crude **16** was treated with CH_3OH and then filtered. The filtrate was concentrated to dryness and the crude was purified by flash chromatography on silica gel (CH_2Cl_2/CH_3OH 9/1 → 8/1) to give compound **16** in 69% yield over 2 steps as a pale yellow sticky solid. $[\alpha]_D^{25}$ = - 11.2 (c 0.52, CH_3OH); ^1H NMR (200 MHz, CD_3OD) δ: 8.32 (d, *J* = 9.2 Hz, 2H), 7.39 (d, *J* = 9.2 Hz, 2H), 4.26 (d, *J* = 7.9 Hz, 1H), 3.94-3.87 (m, 2H), 3.70-3.67 (m, 1H), 3.57-3.53 (m, 1H), 3.38-3.25 (m, 3H), 3.22-3.17 (m, 3H), 2.69 (t, *J* = 7.0 Hz, 2H), 1.93 (t, *J* = 6.9 Hz, 2H), 1.83-1.72 (m, 4H), 1.67-1.61 (m, 2H), 1.56-1.51 (m, 2H), 1.46-1.35 (m, 4H). ^{13}C NMR (50 MHz, CD_3OD) δ: 175.4, 172.4, 156.9, 146.6, 126.0, 123.8, 104.2, 78.0, 77.8, 75.0, 71.6, 70.6, 62.7, 40.3, 36.6, 34.5, 30.6, 30.3, 27.7, 26.7, 26.3, 25.2. HRMS: (m/z) calcd for $[M+H]^+$ $C_{24}H_{37}N_2O_{11}$ 529.23919, found 529.23949.

Synthesis of glucose coated MNPs (GlcMNPs)

In the first step magnetite MNPs were synthesized as follows: A solution of iron (III) acetylacetonate (0.3518 g, 1.00 mmol), oleylamine (0.941 g, 3.52 mmol) and oleic acid (1.2802 g, 4.53 mmo6l) in benzyl ether (25 mL) was stirred at rt under nitrogen flow for 15'. The reaction mixture was heated to 200°C at a rate of 12 °C/min and maintained at that temperature for 20'. The solution was then heated to reflux (ca. 300°C) at a rate of 10 °C/min and stirred for further 15' and finally cooled to rt. The mixture was diluted with hexane (20 mL) and ethanol was added in order to precipitate the magnetic nanoparticles with the assistance of a permanent magnet. The obtained black product was washed with ethanol and then dried under vacuum (53 mg).

The as obtained product (20.6 mg) was mixed with a water solution of tetramethylammonium hydroxide (TMAOH, 25 mL 7% m/m) and sonicated for 10'. MNPs were precipitated adding a 10:1 isopropanol/hexane solution with the assistance of a permanent magnet. The same procedure was repeated three times. Finally, MNPs were washed twice with ethanol and dried under vacuum. The fine powder product (**MNP-TMAOH**) was dissolved in water (20 mL) and purified by dialysis in cellulose membrane.

In the second step the MNPs were coated with 3-aminopropyl phosphonic acid (APPA) by ligand exchange: the pH of a water dispersion of **MNP-TMAOH** (20 mL, 1mg/mL) was increased to ca. 8 with 0.1 M NaOH and then APPA (100 mg, 0.72 mmol) was addedd. The reaction mixture was sonicated for 5' and kept under mechanical stirring for 96 h. APPA coated MNPs (**MNP-APPA**) were magnetically decanted, washed twice with water and dispersed in DMF (10 mL).

Finally, a solution of **16** (9.6 mg, 0.018 mmol) in DMF (1 mL) was added to a solution of **MNP-APPA** in DMF (10 mL, 2 mg/mL). The mixture was sonicated for 5' and then kept under mechanical stirring for 24h. MNPs were recovered using a permanent magnet and washed with

water and with methanol. The final product was dried under vacuum and dispersed in water (10 mL).

Average size of the **GMNPs** obtained by TEM analysis: 12.4 ± 1.7 nm; The XRD pattern matches that expected for a cubic spine ferrite (lattice parameter, a = 8.3913(7); crystallite average diameter, estimated from Scherrer analysis d = 10.8 nm). Saturation Magnetization at 300 K = 70 emu/g.

Synthesis of PEG coated MNPs (PEMNPs)

A toluene solution of MNPs obtained following the same procedure described above (2 mL, 10 mg/mL) was diluted in hexane (50 mL) and mixed with a solution of methoxy(polyethylenoxy)propyltrimethoxysilane 9-12 PE units (300 µL) in a 5:1 hexane/chloroform solution (30 mL). Glacial acetic acid (8 µL, 0.14 mmol) was added to the reaction mixture and the solution was stirred at rt for 15h. MNPs were separated from the supernatant. The product was washed with chloroform and precipitated with hexane with the assistance of a permanent magnet. After the washing step the as obtained PEMNPs were dispersed in water (10 mL).

Average size of the NP obtained by TEM analysis: 12.5 ± 1.6 nm; The XRD pattern matches that expected for a cubic spine ferrite (lattice parameter, a = 8.3924(9); crystallite average diameter, estimated from Scherrer analysis d = 10.7 nm). Saturation Magnetization at 300 K = 80 emu/g.

Spectroscopic data and optical rotations

Compound 4: m.p.: 173-175°C; $[\alpha]_D^{25} = +89.3$ (c 0.75, $CHCl_3$); ^1H NMR (400 MHz, $CDCl_3$) δ: 7.41-7.32 (m, 5H, Ph), 5.97 (bs, 1H, NH), 5.66 (d, $J_{1,2} = 2.8$ Hz, 1H, H_1), 5.42 (dd, $J_{4,3} = 3.2$

Hz, $J_{4,5}$ = 1.2 Hz, 1H, H_4), 5.26-5.23 (A part of an AB system, J_{AB} = 12.0 Hz, 1H, CH_2Ph), 5.22-5.19 (B part of an AB system, J_{BA} = 12.0 Hz, 1H, CH_2Ph), 5.06 (dd, $J_{3,2}$ = 11.6 Hz, $J_{3,4}$ = 2.8 Hz, 1H, H_3), 4.43 (at, J = 6.8 Hz, 1H, H_5), 4.43-4.34 (m, 1H, $H_{5'}$), 4.14-4.13 (m, 2H, H_{6a}, H_{6b}), 3.62 (dd, $J_{2,3}$ = 11.6 Hz, $J_{2,1}$ = 2.4 Hz, 1H, H_2), 2.91-2.85 (A part of an ABX system, J_{AB} = 17.6 Hz, J_{AX} = 6.0 Hz, 1H, $H_{4a'}$), 2.83-2.75 (B part of an ABX system, J_{BA} = 16.8 Hz, J_{BX} = 11.2 Hz, 1H, $H_{4b'}$), 2.16 (s, 3H, COCH_3), 2.06 (s, 3H, COCH_3), 2.02 (s, 3H, COCH_3); ^{13}C NMR (100 MHz, $CDCl_3$) δ: 170.5 (Cq), 170.1 (Cq), 169.9 (Cq), 169.1 (Cq), 164.3 (Cq), 154.0 (Cq), 134.7 (Cq), 129.0 (CH, Ph), 128.9 (CH, Ph), 128.6 (CH, Ph), 98.2 (Cq), 95.9 (C_1), 69.1 (C_5), 68.1 (CH$_2$Ph), 67.2 (C_4), 65.7 (C_3), 61.6 (C_6), 51.5 ($C_{5'}$), 36.6 (C_2), 30.9 ($C_{4'}$), 20.8 (COCH$_3$), 20.7 (COCH$_3$); ESI-MS: m/z 571.84 $[M+Na]^+$, 585.83 $[M+K]^+$; Elemental Analysis for $C_{25}H_{27}NO_{11}S$: calc. C 54.64, H 4.95, N 2.55; found C 54.32, H 4.80, N 2.68.

Compound 7: $[\alpha]_D^{25}$: + 84.3 (c 0.65, $CHCl_3$); ^{1}H NMR (400 MHz, $CDCl_3$) δ: 7.56-7.54 (m, 1H, CONHCH$_2$), 6.99 (d, J = 2.8 Hz, 1H, CONHCH), 5.68 (d, $J_{1,2}$ = 2.8 Hz, 1H, H_1), 5.42 (dd, $J_{4,3}$ = 3.1 Hz, $J_{4,5}$ = 1.3 Hz, 1H, H_4), 5.00 (dd, $J_{3,2}$ = 11.6 Hz, $J_{3,4}$ = 2.8 Hz, 1H, H_3), 4.44 (at, J = 6.8 Hz, 1H, H_5), 4.22 (atd, J = 6.8 Hz, J = 2.4 Hz, 1H, $H_{5'}$), 4.17-4.00 (m, 2H, H_{6a}, H_{6b}), 3.74-3.50 (m, 24H, CH_2O, H_2, $H_{1''}$), 3.44-3.36 (m, 1H, $H_{1''}$), 2.99-2.93 (A part of an ABX system, J_{AB} = 16.7 Hz, J_{AX} = 7.3 Hz, 1H, $H_{4a'}$), 2.92-2.86 (B part of an ABX system, J_{BA} = 16.7 Hz, J_{BX} = 6.9 Hz, 1H, $H_{4b'}$), 2.79 (bs, 1H, OH), 2.16 (s, 3H, COCH_3), 2.06 (s, 3H, COCH_3), 2.02 (s, 3H, COCH_3); ^{13}C NMR (50 MHz, $CDCl_3$) δ: 170.4 (Cq), 170.2 (Cq), 170.0 (Cq), 169.9 (Cq), 164.3 (Cq), 154.8 (Cq), 97.5 (Cq), 96.0 (C_1), 72.9 (CH$_2$O), 70.7 (CH$_2$O), 70.4 (CH$_2$O), 69.6 (CH$_2$O), 69.1 (C_5), 67.4 (C_4), 66.2 (C_3), 61.8 (C_6), 61.7 ($C_{12''}$), 52.4 ($C_{5'}$), 40.0 ($C_{1''}$), 36.6 (C_2), 31.0 ($C_{4'}$), 20.7 (COCH$_3$); ESI-MS**:** *m/z* 745.28 $[M+Na]^+$; Elemental Analysis for $C_{30}H_{46}N_2O_{16}S$: calc. C 49.85, H 6.42, N 3.88; found C 49.79, H 5.68, N 4.22.

Compound 8: $[\alpha]_D^{25}$ = + 70.1 (c = 0.76, $CHCl_3$); ^{1}H NMR (400 MHz, $CDCl_3$) δ: 7.18 (t, *J* = 5.2 Hz, 1H, CON*H*CH_2), 6.73 (d, 1H, *J* = 2.4 Hz, 1H, CON*H*CH), 5.69 (d, $J_{1,2}$ = 2.7 Hz, 1H, H_1), 5.43-5.42 (m, 1H, H_4), 5.01 (dd, $J_{3,2}$ = 11.6 Hz, $J_{3,4}$ = 3.2 Hz, 1H, H_3), 4.44 (at, *J* = 6.4 Hz, 1H, H_5), 4.19-4.13 (m, 3H, $H_{5'}$, H_{6a}, H_{6b}), 3.80-3.76 (m, 3H, CH_2O), 3.75-3.58 (m, 18H, CH_2O, H_2), 3.49-3.45 (m, 4H, $H_{12''}$, $H_{1''}$), 3.00-2.94 (A part of an ABX system, J_{AB} = 16.7 Hz, J_{AX} = 7.4 Hz, 1H, $H_{4a'}$), 2.92-2.86 (B part of an ABX system, J_{BA} = 16.7 Hz, J_{BX} = 6.8 Hz, 1H, $H_{4b'}$), 2.16 (s, 3H, COCH_3), 2.07 (s, 3H, COCH_3), 2.02 (s, 3H, COCH_3); ^{13}C NMR (100 MHz, $CDCl_3$) δ: 170.4 (Cq), 170.0 (Cq), 169.9 (Cq), 164.2 (Cq), 154.6 (Cq), 97.3 (Cq), 95.7 (C_1), 71.1 (*C*H_2O), 70.5 (*C*H_2O), 70.44 (*C*H_2O), 70.41 (*C*H_2O), 70.39 (*C*H_2O), 70.36 (*C*H_2O), 70.30 (*C*H_2O), 69.4 (*C*H_2O), 68.9 (C_5), 67.1 (C_4), 66.0 (C_3), 61.5 (C_6), 52.2 ($C_{5'}$), 39.9 ($C_{1''}$), 36.3 (C_2), 30.7 ($C_{4'}$), 30.4 ($C_{12''}$), 20.68 (CO*C*H_3), 20.63 (CO*C*H_3), 20.5 (CO*C*H_3); ESI-MS: *m/z* 785.31 $[M+H]^+$, 807.49 $[M+Na]^+$; Elemental Analysis for $C_{30}H_{45}BrN_2O_{15}S$: calc. C 45.86, H 5.77, N 3.57; found C 46.23, H 5.82, N 3.17.

Compound 9: $[\alpha]_D^{25}$ = + 77.9 (c 0.28, MeOH); ^{1}H NMR (400 MHz, $CDCl_3$) δ: 8.33 (bs, 1H, CON*H*CH), 7.80 (bs, 1H, CON*H*CH_2), 5.70 (d, $J_{1,2}$ = 2.8 Hz, 1H, H_1), 5.41 (bs, 1H, H_4), 4.98 (dd, $J_{3,2}$ = 11.6 Hz, $J_{3,4}$ = 3.0 Hz, 1H, H_3), 4.44 (at, *J* = 6.5 Hz, 1H, H_5), 4.22-4.13 (m, 3H, $H_{5'}$, H_{6a}, H_{6b}), 3.84-3.46 (m, 25H, CH_2O, H_2, $H_{1''}$, $H_{11''}$, O*H*, O*H*), 3.07-3.01 (A part of an ABX system, J_{AB} = 16.8 Hz, J_{AX} = 6.0 Hz, 1H, $H_{4a'}$), 2.98-2.92 (B part of an ABX system, J_{BA} = 16.8 Hz, J_{BX} = 7.3 Hz, 1H, $H_{4b'}$), 2.18-2.10 (m, 2H, $H_{12''}$), 2.15 (s, 3H, COCH_3), 2.06 (s, 3H, COCH_3), 2.02 (s, 3H, COCH_3); ^{13}C NMR (50 MHz, $CDCl_3$) δ: 170.4 (Cq), 170.2 (Cq), 169.9 (Cq), 169.8 (Cq), 165.8 (Cq), 156.1 (Cq), 96.1 (Cq), 95.8 (C_1), 70.3 (*C*H_2O), 69.9 (*C*H_2O), 69.7 (*C*H_2O), 69.3 (*C*H_2O), 68.8 (C_5), 67.1 (C_4), 65.9 (C_3), 65.2 (*C*H_2O), 61.5 (C_6), 51.8 ($C_{5'}$), 39.7 ($C_{1''}$), 36.1

(C_2), 29.9 (C4'), 27.79 (d, $J_{C\text{-}P}$ = 137.2 Hz, $C_{12''}$), 20.6 ($CO\mathit{C}H_3$); ^{31}P NMR (81 MHz, $CDCl_3$) δ: 29.84 (s); HRMS**:** (*m/z*) calcd for $[M+H]^+$ $C_{30}H_{48}O_{18}N_2PS$ 787.23550, found 787.23590.

Compound 2: ^{1}H NMR (400 MHz, CD_3OD) δ: 5.68 (d, $J_{1,2}$ = 2.8 Hz, 1H, H_1), 4.24 (at, J = 6.7 Hz, 1H, $H_{5'}$), 4.04 (at, J = 5.9 Hz, 1H, H_5), 3.97 (bs, 1H, H_4), 3.78-3.71 (m, 4H, H_{6a}, H_{6b}, CH_2O), 3.65-3.56 (m, 19H, CH_2O, H_3), 3.47-3.40 (m, 3H, $H_{1''}$, H_2), 2.99-2.93 (A part of ABX system, J_{AB} = 16.8 Hz, J_{AX} = 6.8 Hz, 1H, $H_{4a'}$), 2.81-2.75 (B part of ABX system, J_{BA} = 16.8 Hz, J_{BX} = 6.8 Hz, 1H, $H_{4b'}$), 1.95-1.87 (m, 2H, $H_{12''}$); ^{13}C NMR (50 MHz, CD_3OD) δ: 172.9, 167.6, 157.9, 98.3, 96.6, 74.9, 71.3, 71.1, 70.8, 70.3, 70.2, 68.3, 67.1, 62.5, 53.2, 40.5, 40.4, 31.9, 30.84 (d, $J_{C\text{-}P}$ = 130.5 Hz); ^{31}P NMR (81 MHz, $CDCl_3$) δ: 20.04 (s); HRMS**:** (*m/z*) calcd for $[M+H]^+$ $C_{24}H_{42}O_{15}N_2PS$ 661.20380, found 661.20272.

Copies of NMR spectra

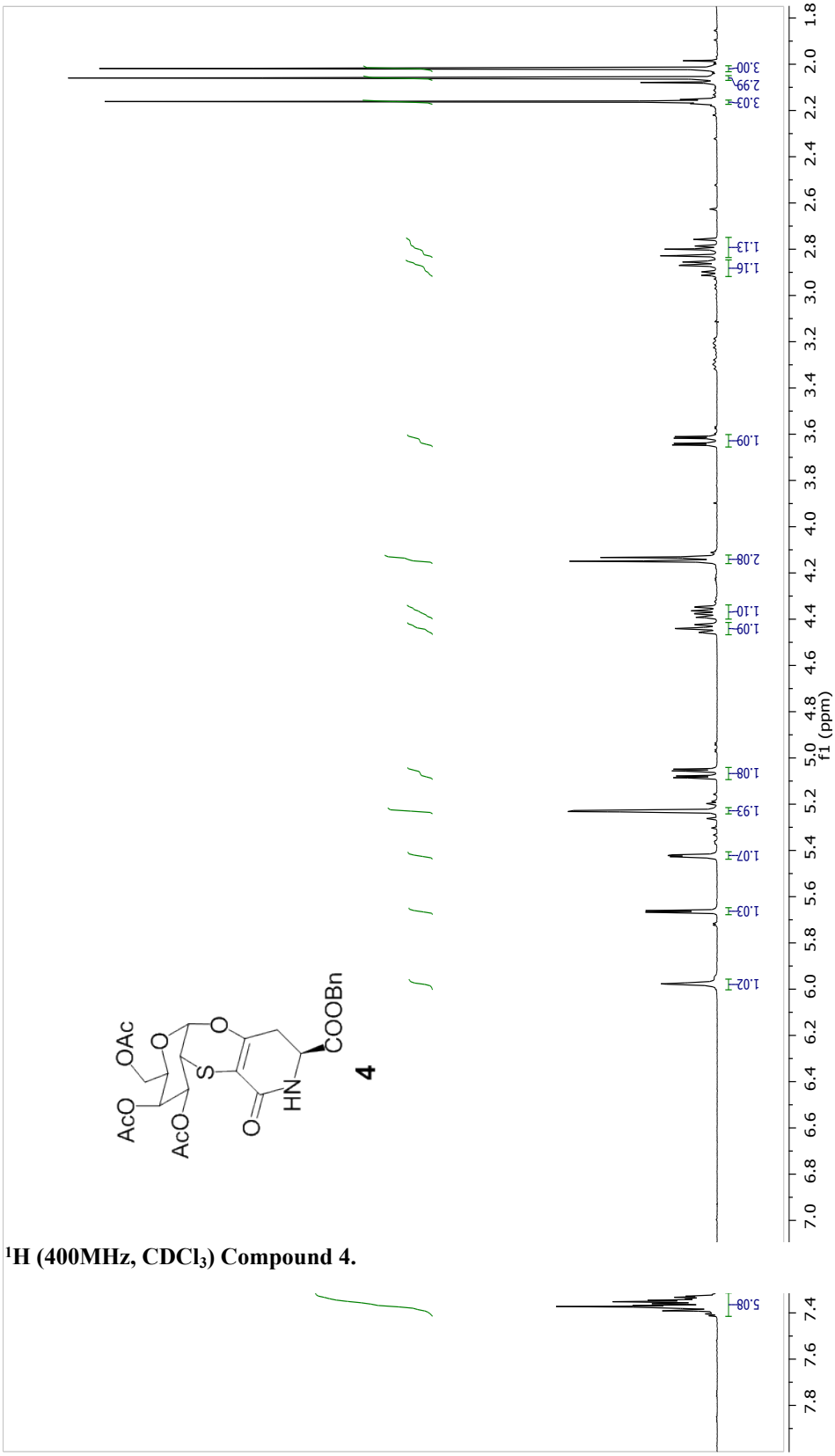

^{1}H (400MHz, $CDCl_3$) Compound 4.

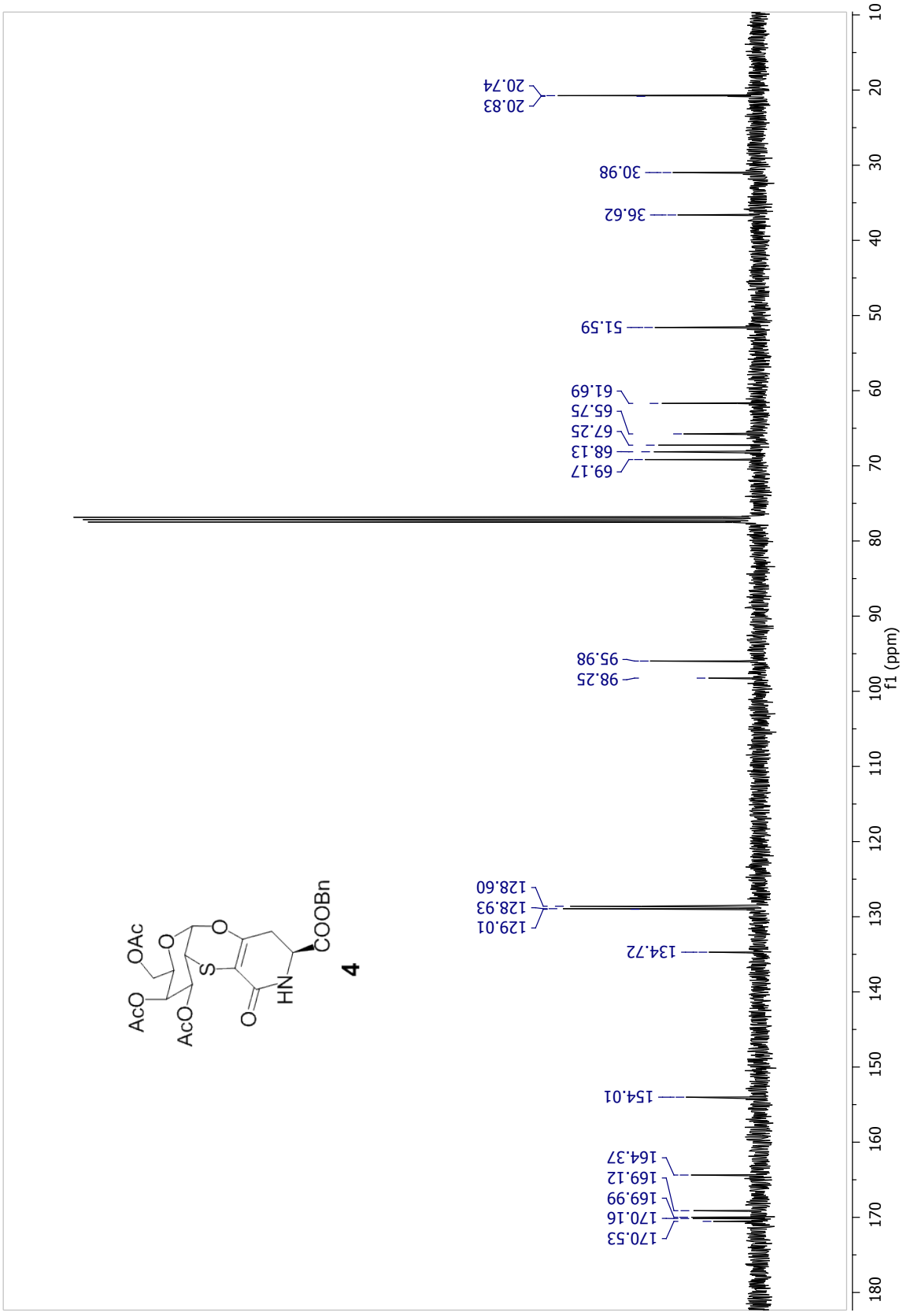

^{13}C (100MHz, $CDCl_3$) Compound 4.

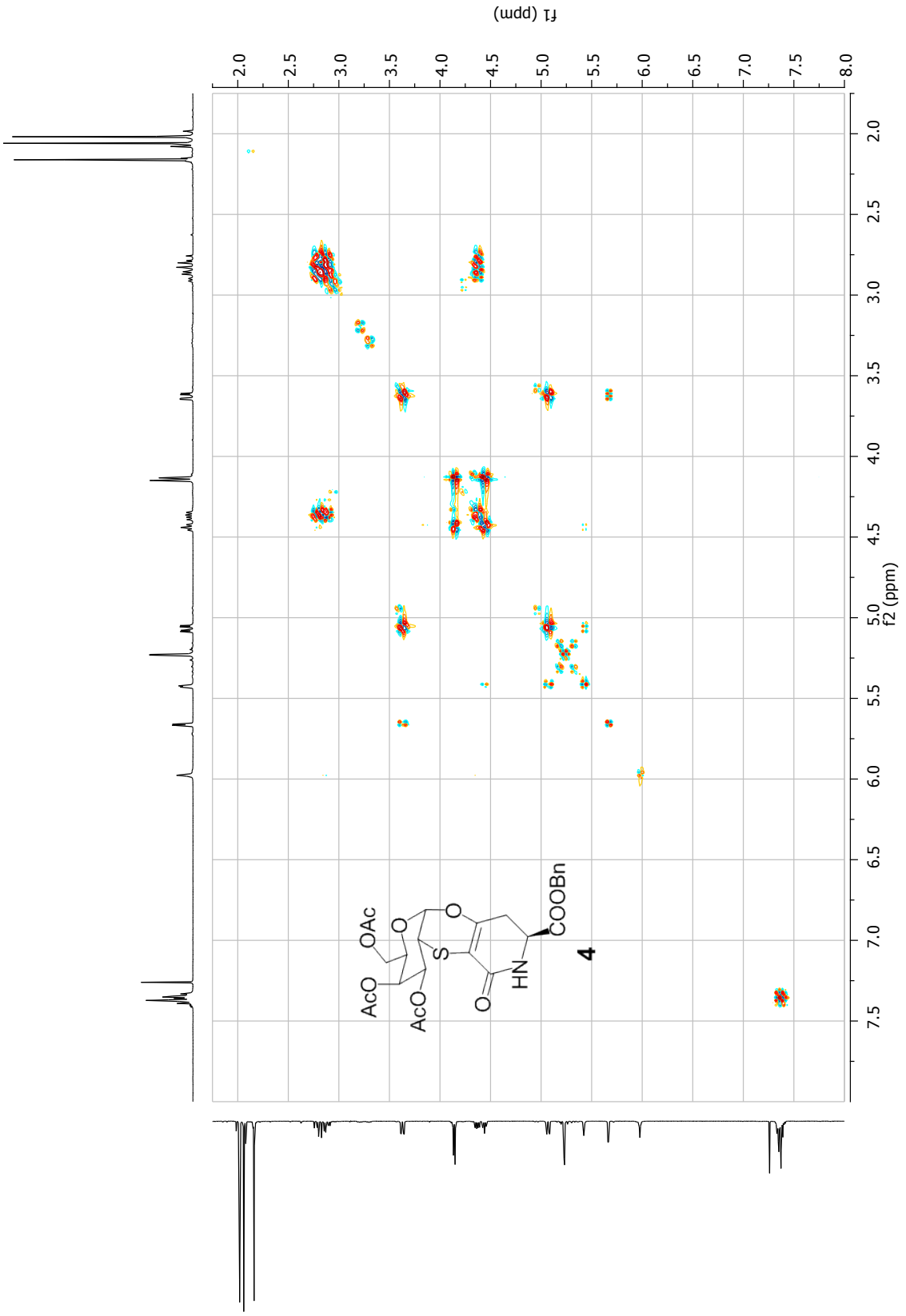

gDQCOSY (400MHz, $CDCl_3$) Compound 4.

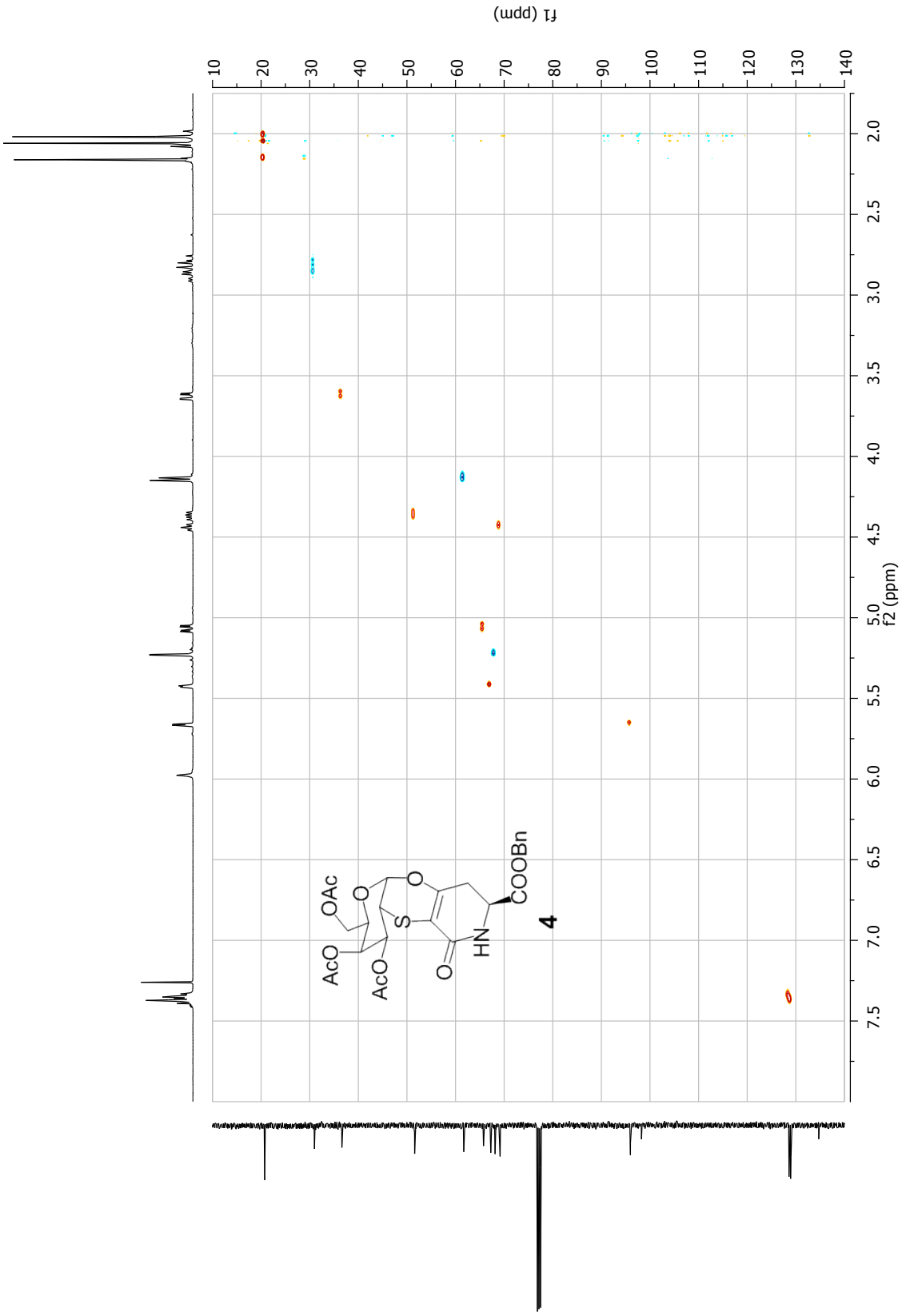

gHSQC (400 MHZ, CDCl3) Compound 4

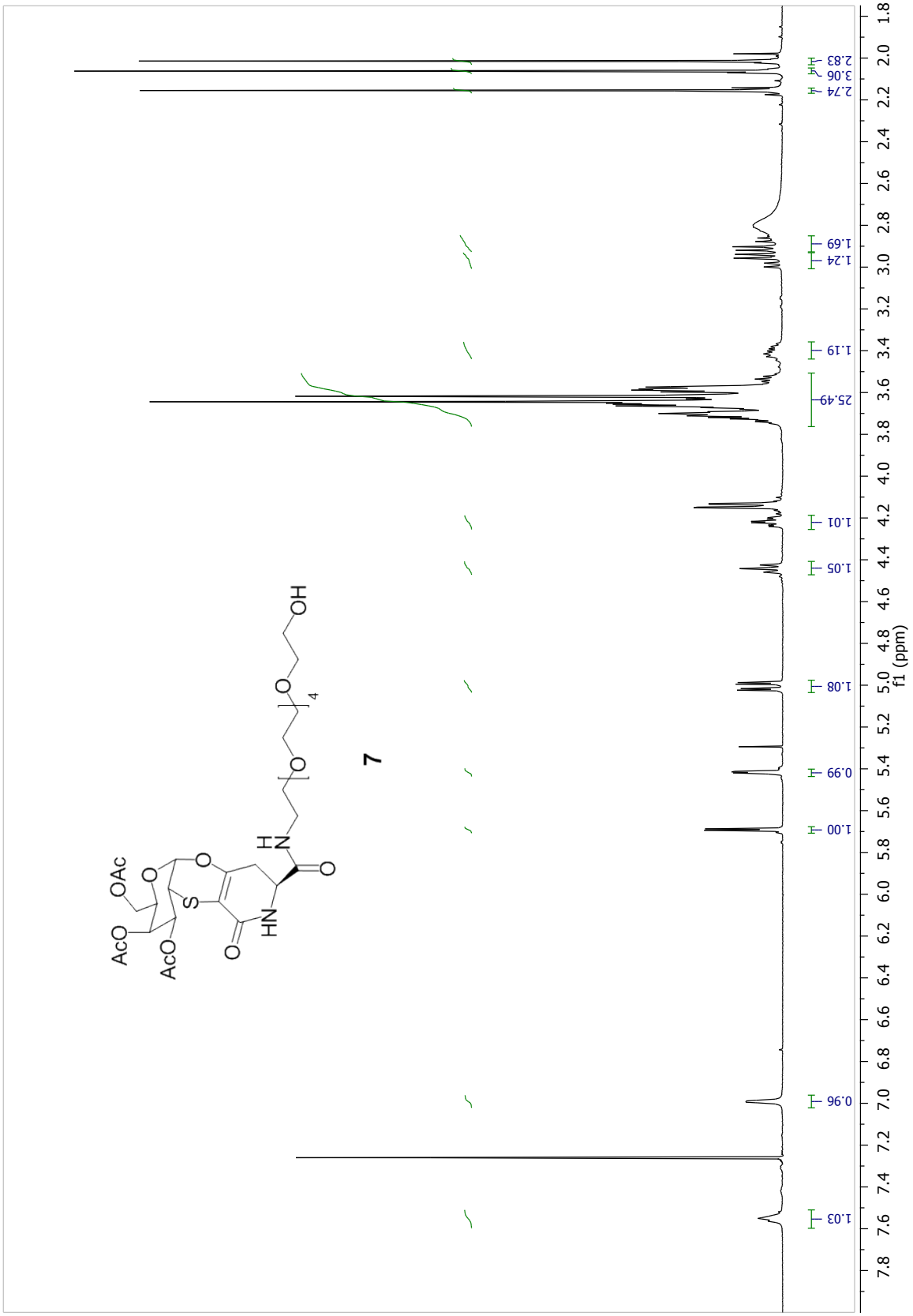

^{1}H (400MHz, $CDCl_3$) Compound 7

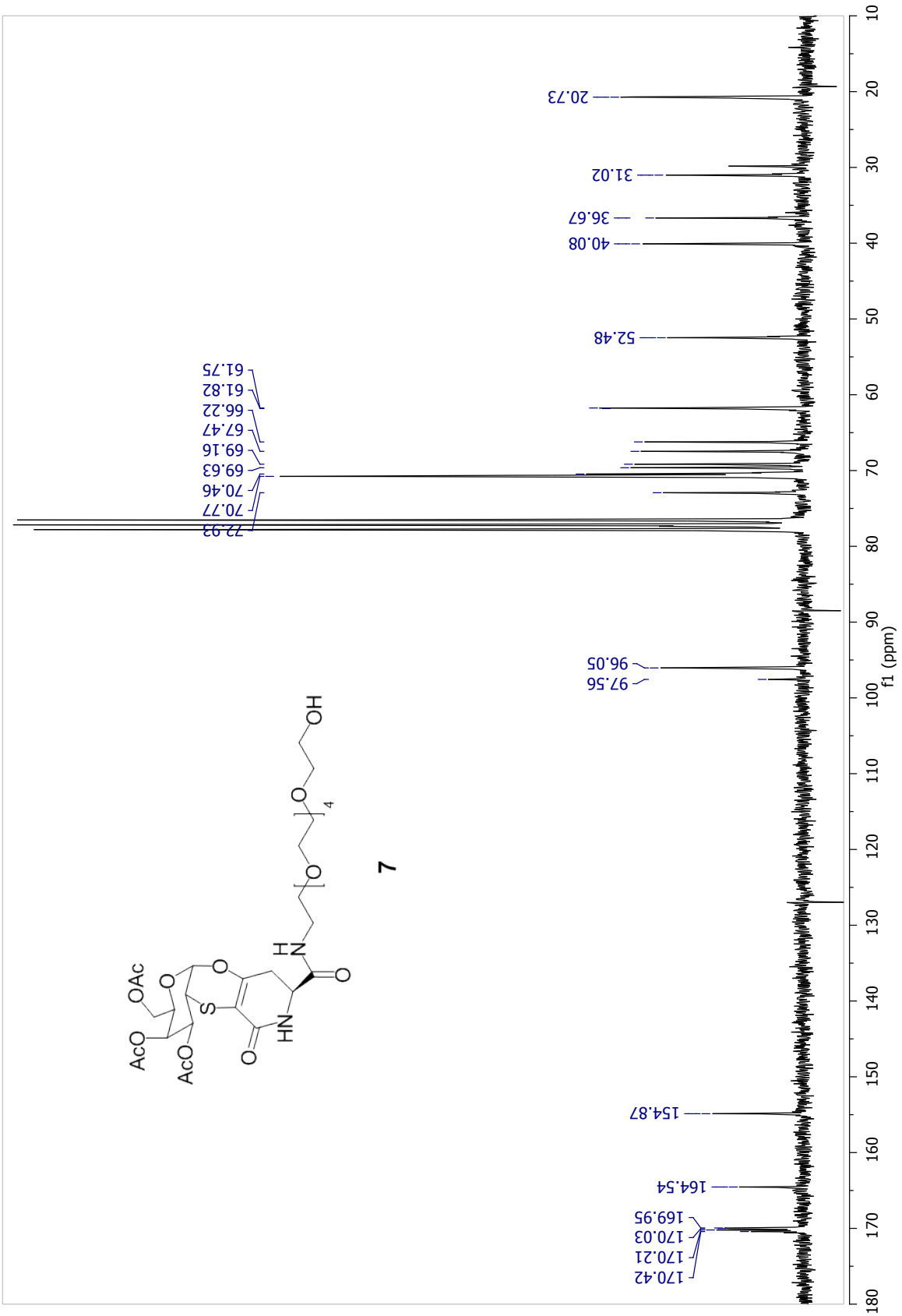

^{13}C (50 MHz, $CDCl_3$) Compound 7

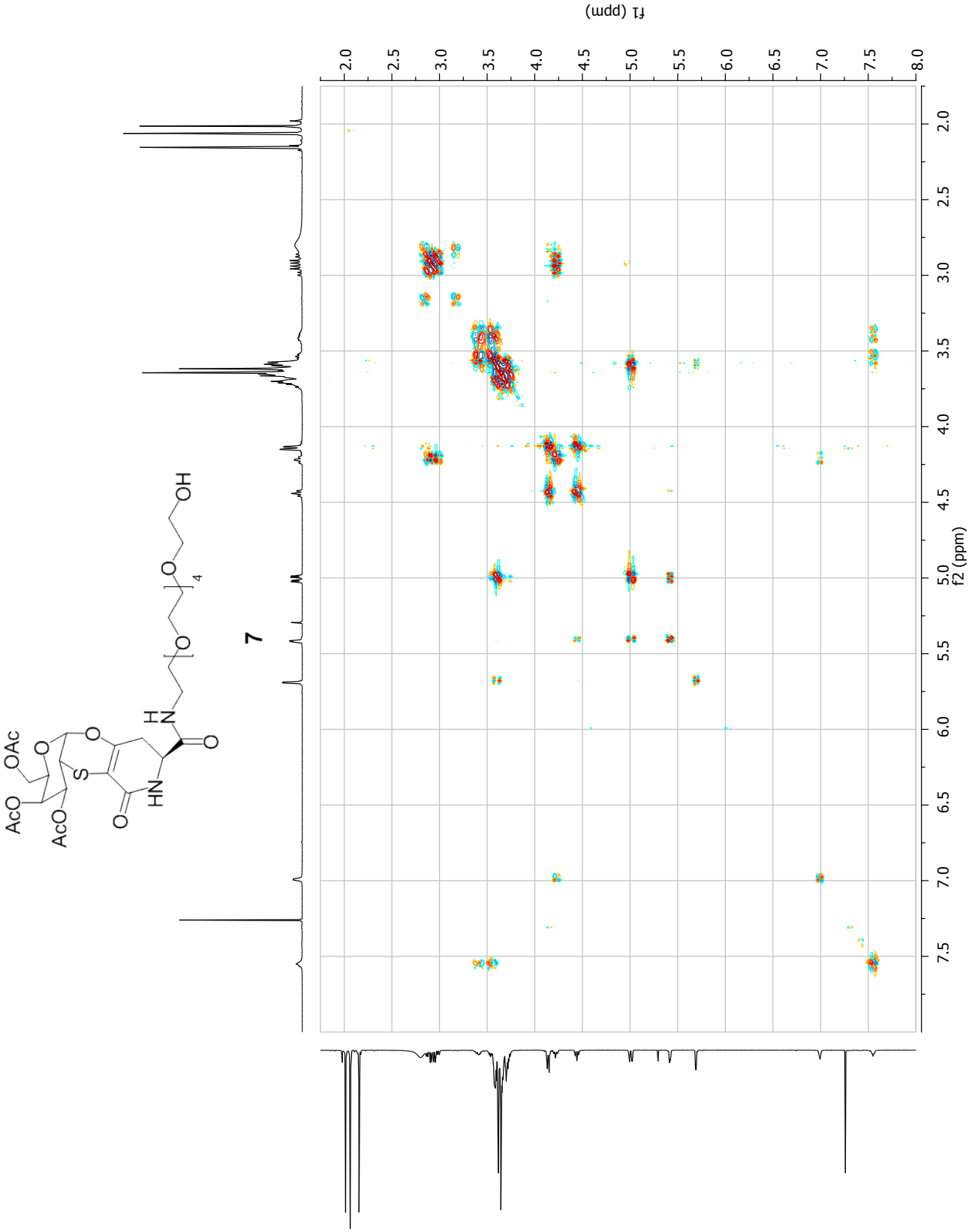

gDQCOSY (400MHz, $CDCl_3$) Compound 7

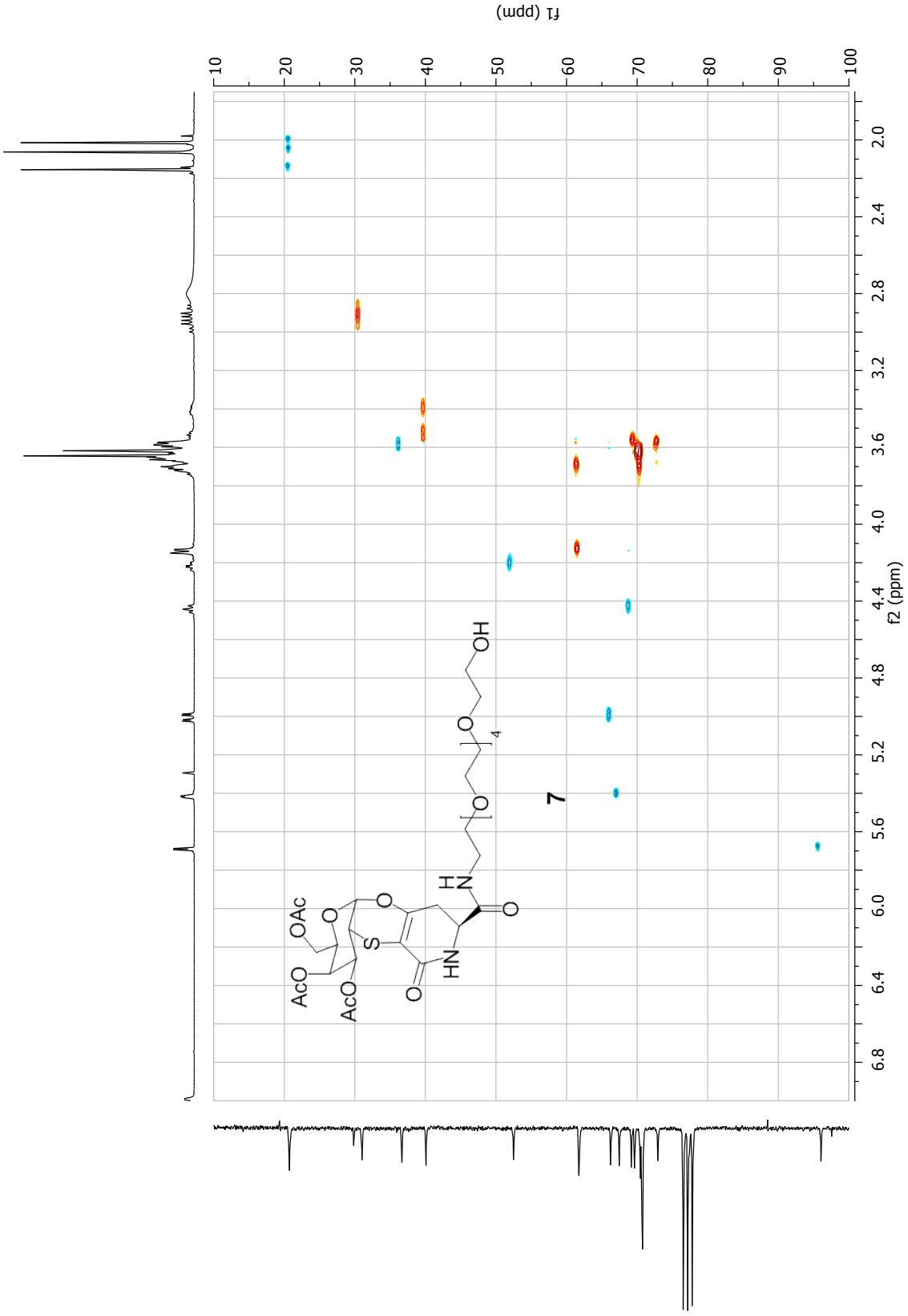

gHSQC (400 MHz, $CDCl_3$) Compound 7

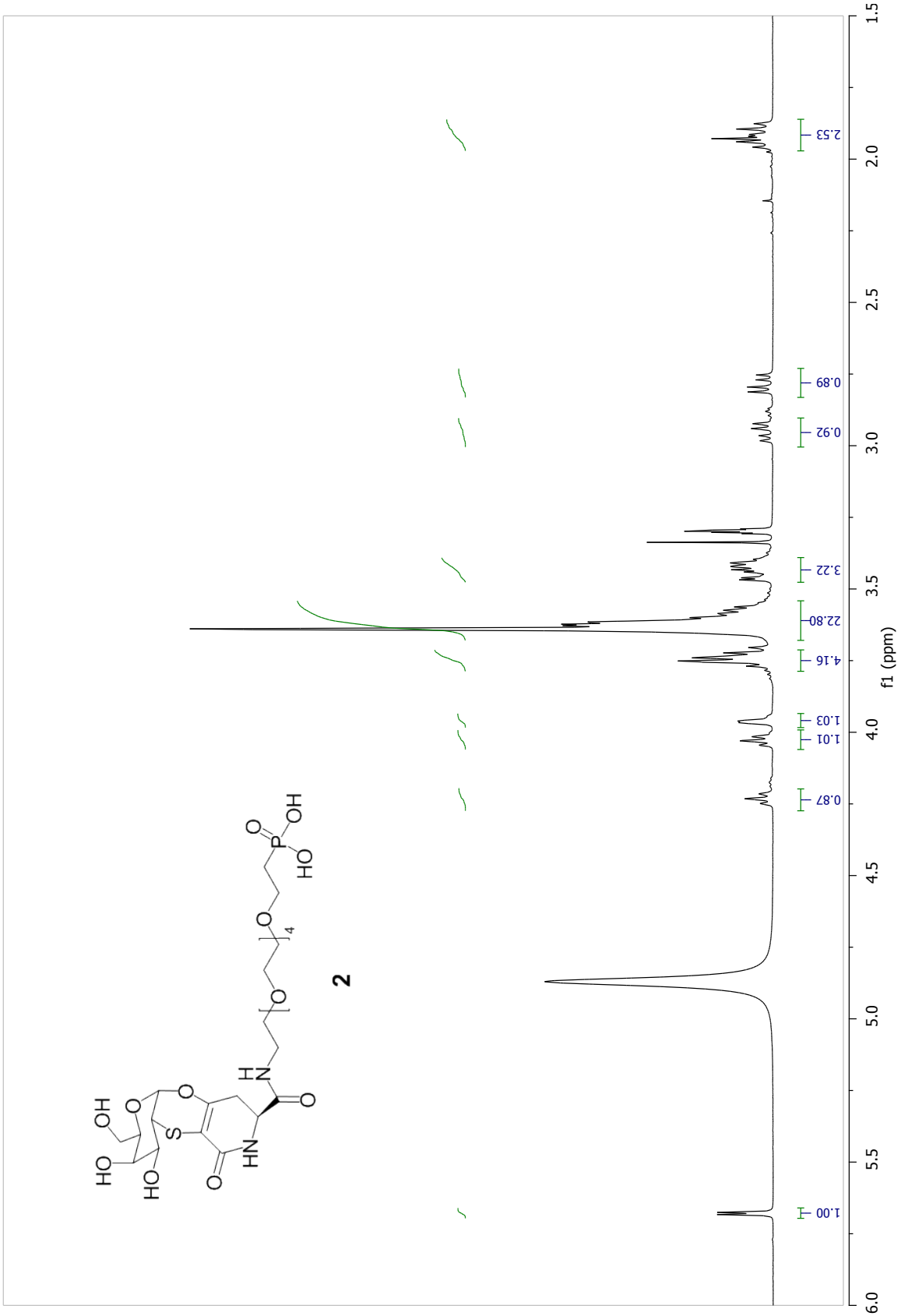

^{1}H (400 MHz, CD_3OD) Compound 2

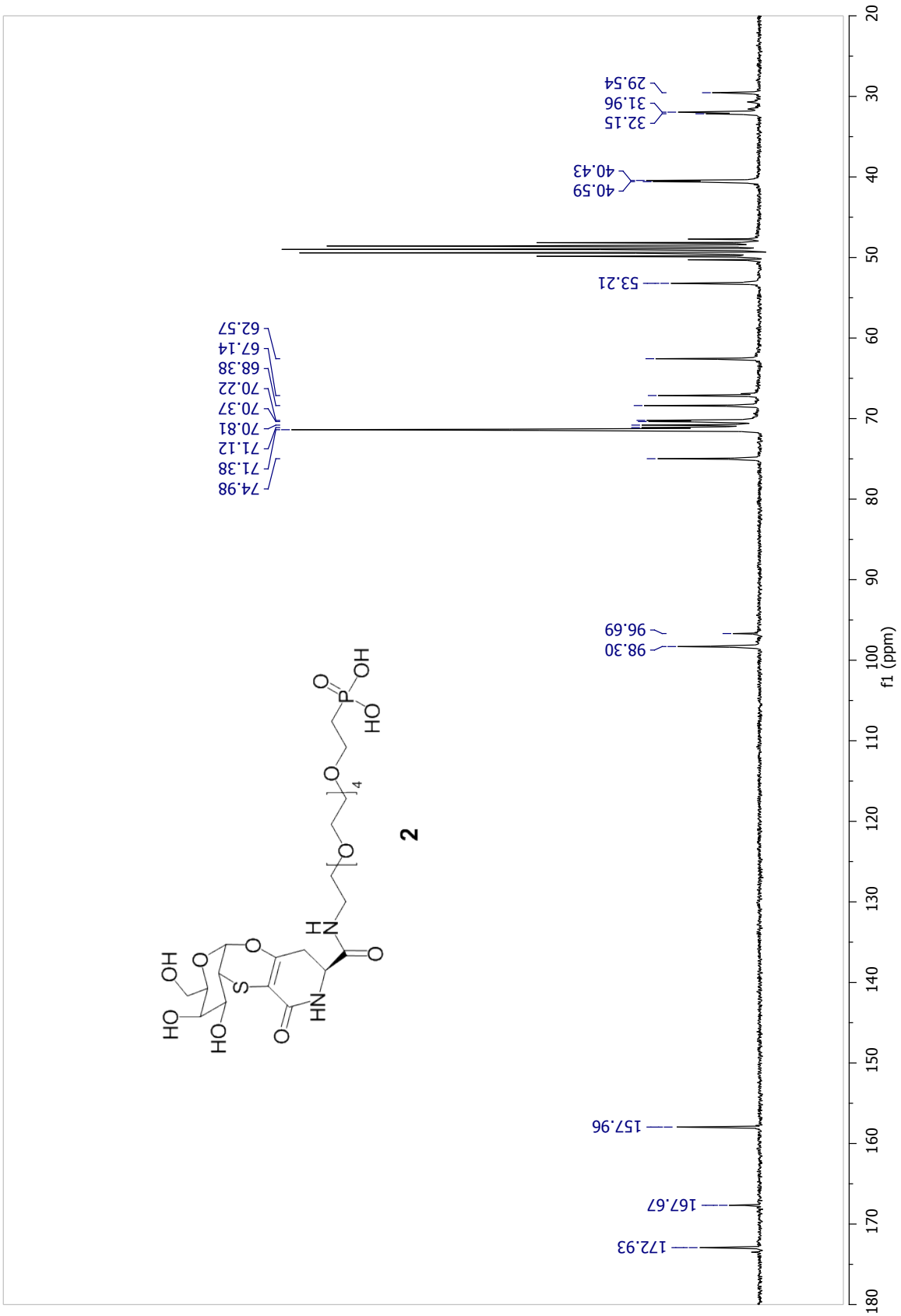

^{13}C (50 MHz, CD_3OD) Compound 2

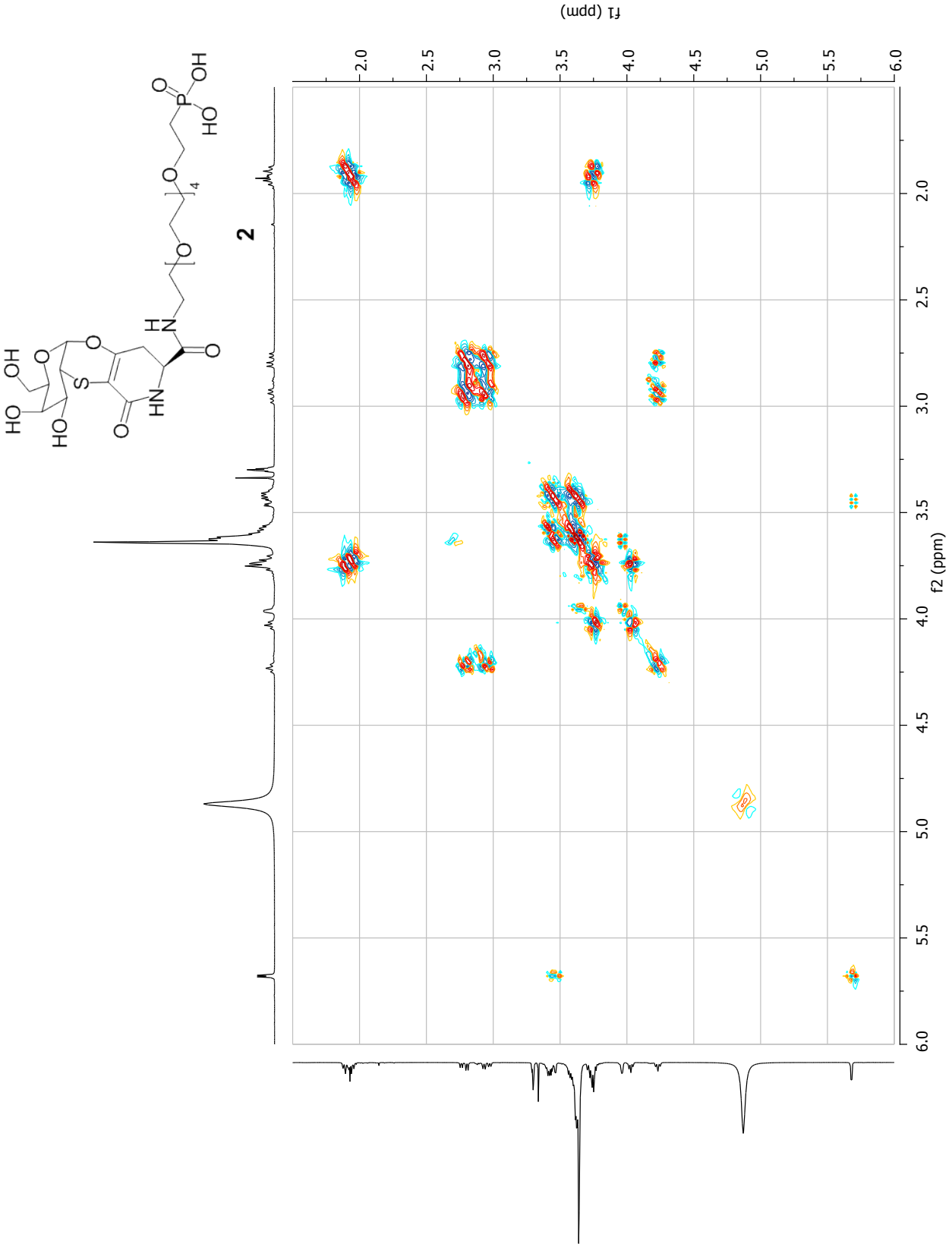

gDQCOSY (400 MHZ, CD_3OD) Compound 2

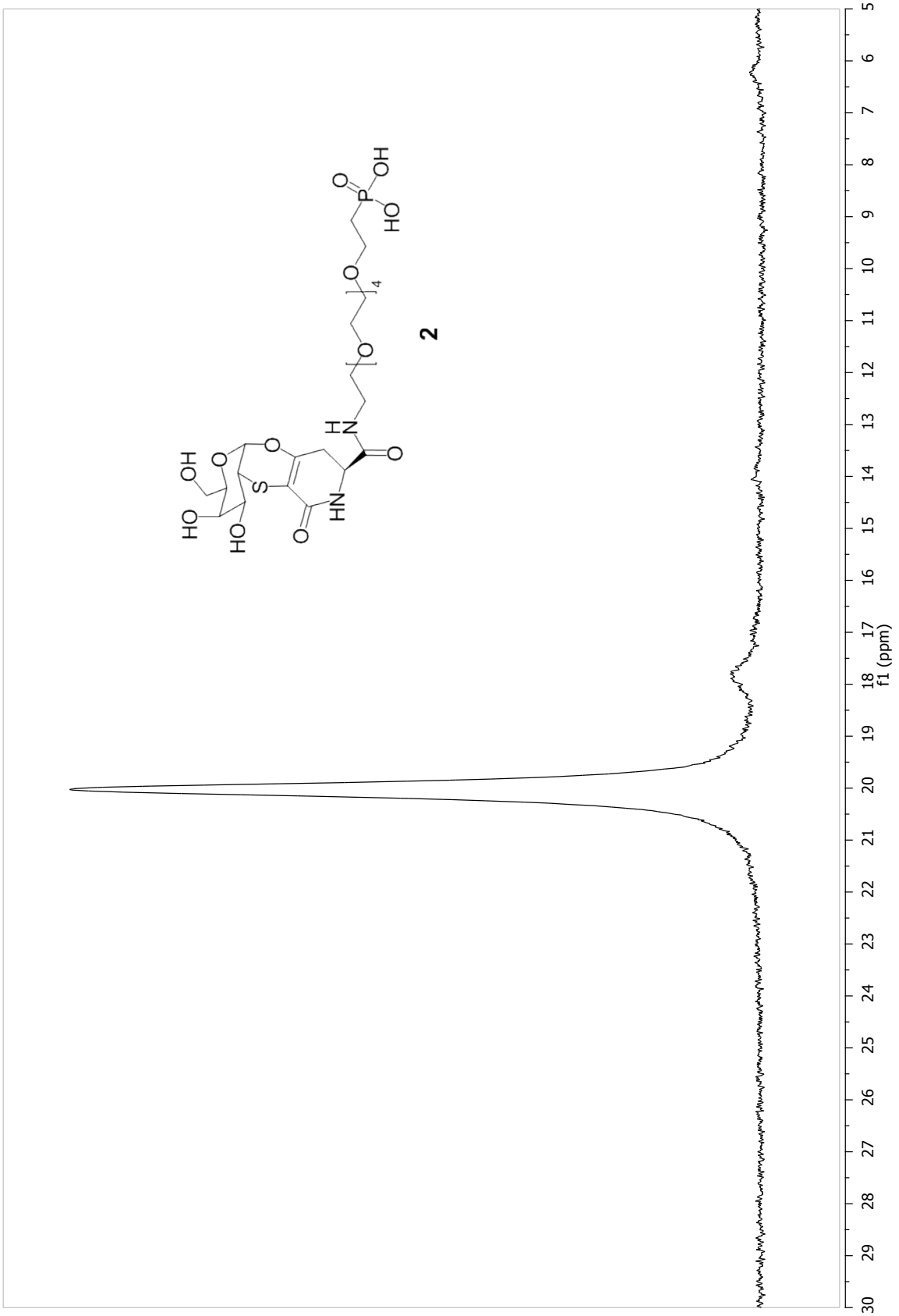

^{31}P (200 MHZ, CD_3OD) Compound 2

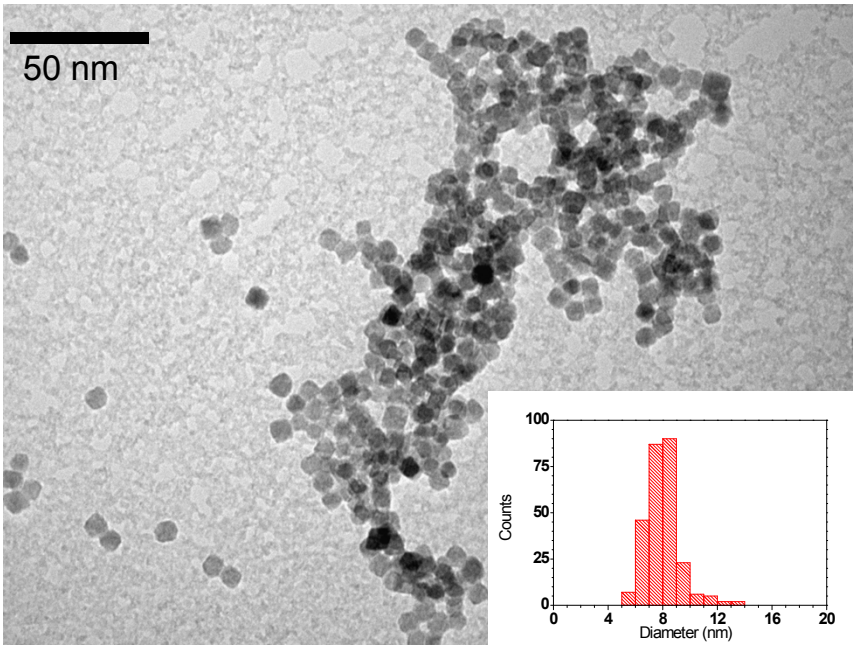

Figure S1: **TEM image of MNP seeds.** Representative bright field low magnification TEM image of MNP before the second reaction step and corresponding particle size distribution. The average size evaluated by statistical analysis over ca. 600 MNP is 7.6 ± 0.7 nm.

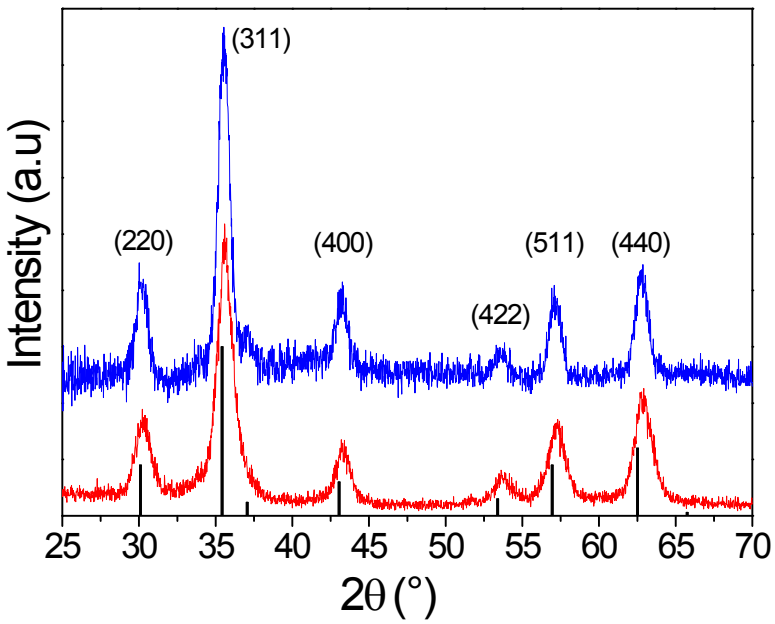

Figure S2: XRD patterns of MNPs. Powder X-Ray Diffraction patterns of MNPs before (red line) and after (blue line) the seed-mediated growth step obtained using Cu Kα radiation. The black bars corresponds to the reference magnetite pattern (JPCDS 19-0629).

The relaxation dynamics of the magnetic moment was further investigated by temperature-dependent AC susceptibility measurements (Figure S3). Both the in- and out-of-phase components of the magnetic susceptibility exhibited frequency-dependent maxima characteristic of a blocking process. The blocking temperatures obtained from the maxima of the out-of-phase component of the magnetic susceptibility, χ", for different observation times $\tau = 1/2\pi\nu$, where ν is the frequency of the ac field, can be effectively fitted to an Arrhenius law, $\tau = \tau_0 \exp(KV/k_BT)$, where K is the magnetic anisotropy energy density, V is the particle volume, τ_0 the attempt time and k_B the Boltzmann constant. The best-fit parameters found were $3\cdot10^{-13} \pm 2\cdot10^{-13}$ s for the pre-exponential factor, τ_0, and 863±18 K for the reversal energy barrier, KV/k_B, which, considering the average volume obtained from the analysis of TEM images, corresponds to $K \approx 2.2\cdot104$ J/m^3. Interestingly, no anomalies in the χ' *vs.* T curves were observed nor at the melting point of heptane (183 K), or at higher temperature, a results which indicates that at room temperature, at least in the investigated time window, the reversal of the magnetization is mainly driven by the Néel mechanism.

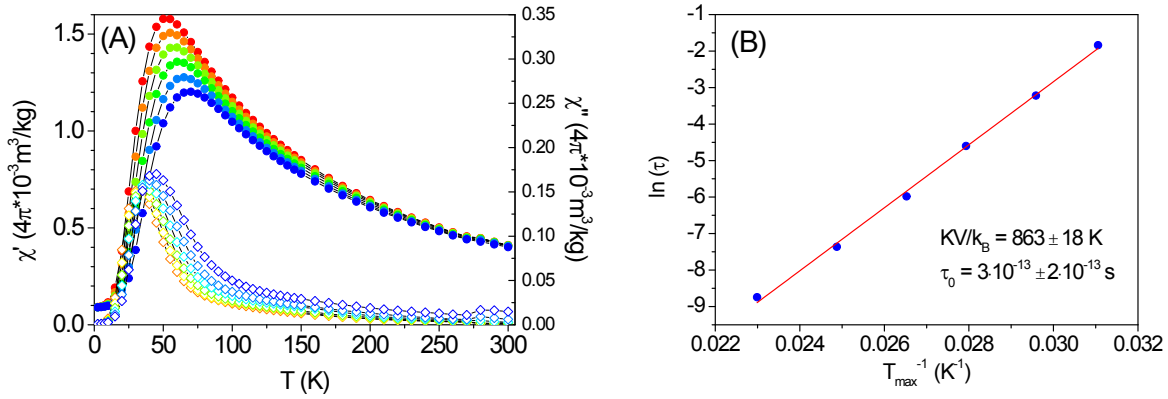

Figure S3: AC susceptibilities and Arrhenius plot. (A) Temperature dependence of in-phase, χ', (full symbols) and out-of-phase, χ", (open symbols) AC susceptibilities. Data were collected

at 6 log-spaced frequencies in the 1-1000 Hz range. (B) Arrhenius plot of the experimental relaxation time and best fit line.

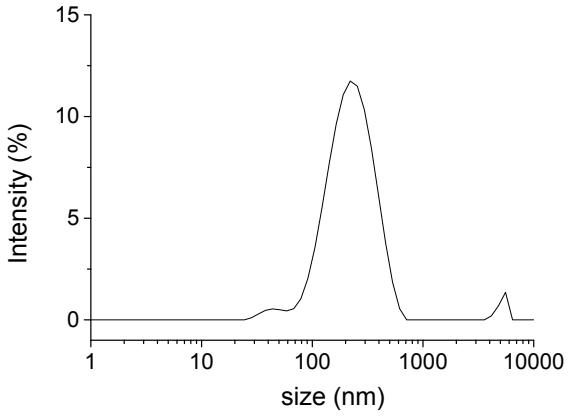

Figure S4 DLS of GMNPs: Size distribution obtained by DLS of MNPs functionalized with the α-Tn mimetic. Although the most part of NPs form aggregates (the average size is 182 nm, polydispersity index = 0.244), the final product appears as a stable colloidal suspension. The Z-potential was -17.4 mV).

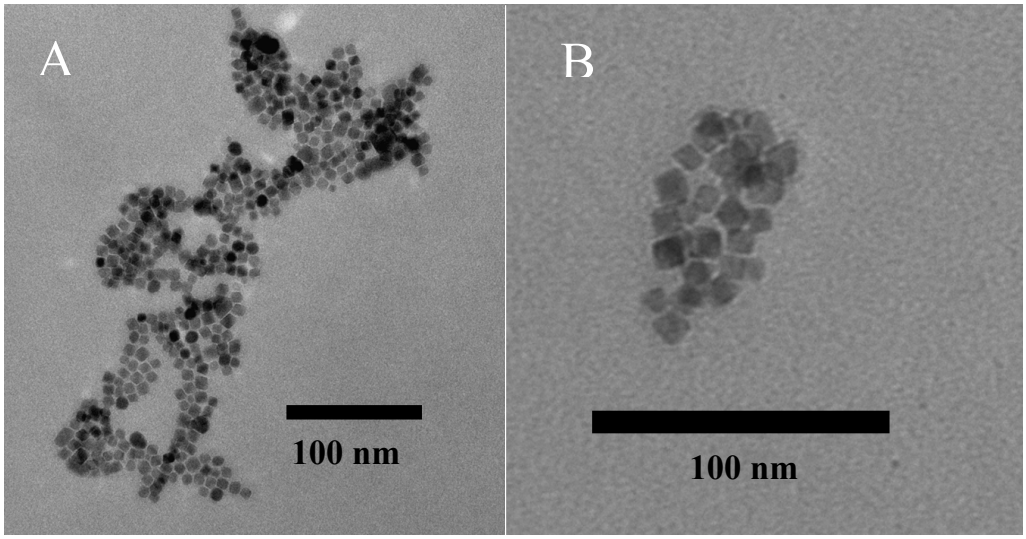

Figure S5: **TEM image of CMNPs and GMNPs.** Representative bright field low magnification TEM images of (A) MNPs functionalized with the α-Tn mimetic antigen and (B) citrate coated MNPs. The size distributions were not affected by the coating processes (d_{ave}=10.7 ± 1.2 and XX ±,yy nm for CMNPs and GMNPs, respectively).

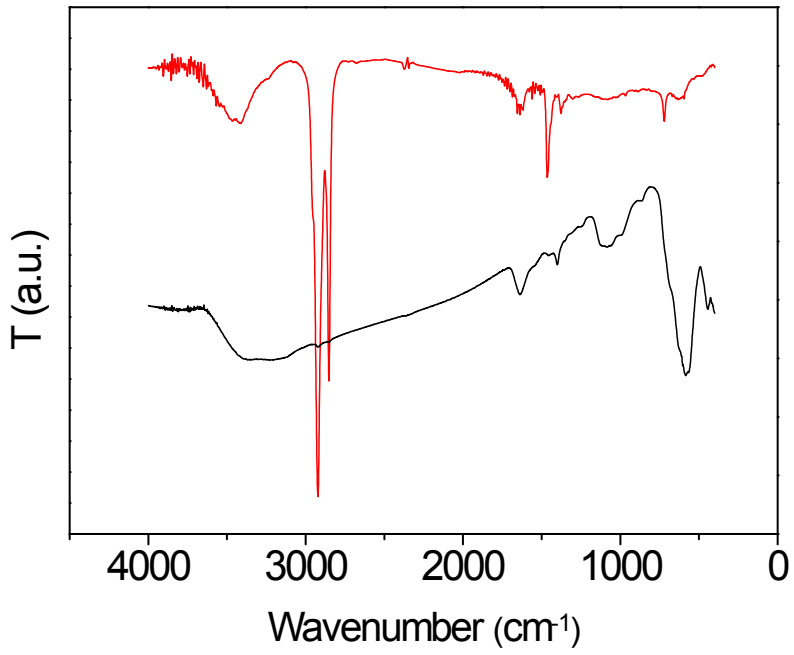

Figure S6: FT-IR spectra of MNPs. FTIR spectra of the MNPs coated with oleic acid (red line) and after the ligand exchange procedure (black).

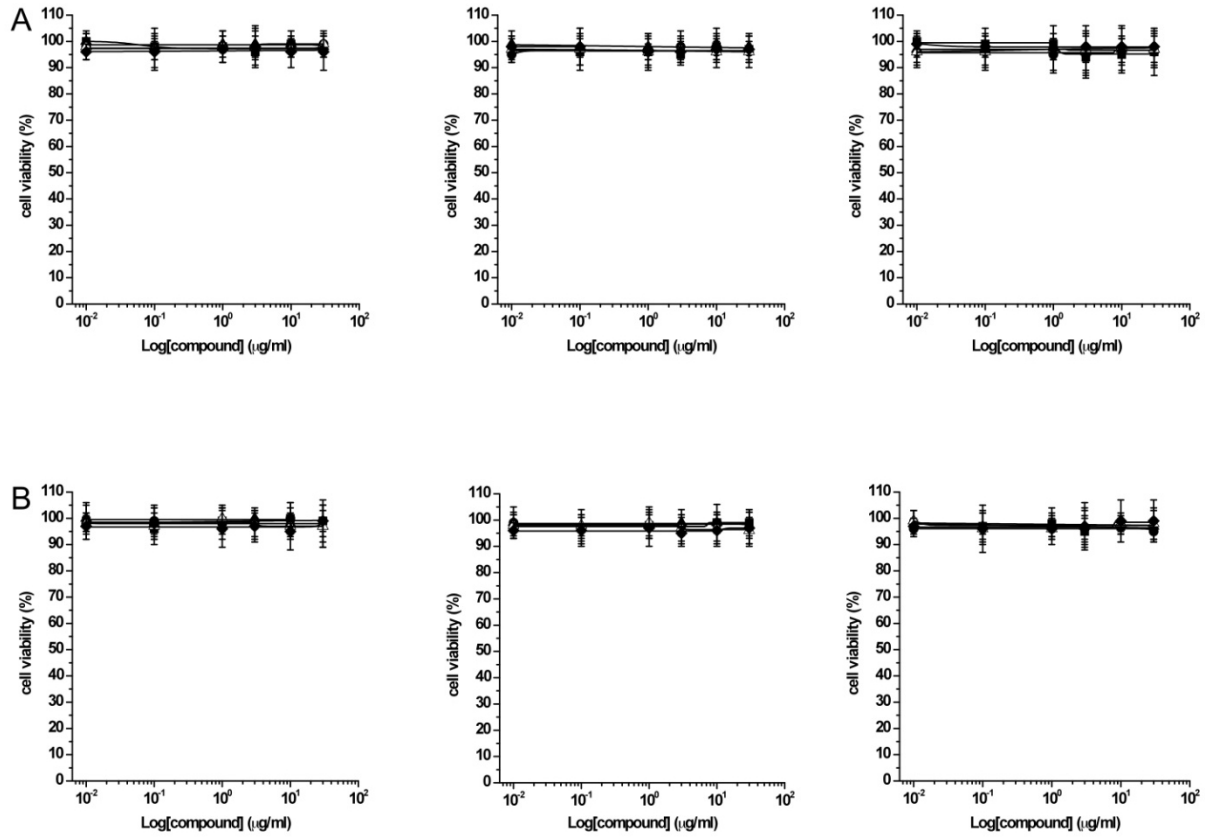

Figure S7: Effects of compound **2**, polyethylene glycol-coated MNPs (**PEMNPs**), citrate-coated MNPs (**CMNPs**), and glycosyl MNPs (**GMNPs** and **GlcMNPs**) on cell viability. RAW 264.7 cells were treated with increasing concentrations (0.01-30 μg/ml) of **2** (closed squares), **PEMNPs** (open triangles), **CMNPs** (closed circles), **GMNPs** (closed triangles) or **GlcMNPs** (closed diamonds) for 24h (left panels), 48h (middle panels) and 72h (right panels). Cell viability was assessed by (A) Calcein-AM assay (B) Trypan Blue exclusion assay. The concentration-response curves show the percentage of cell viability in comparison with controls (untreated cells). The data represent mean ± SEM of at least three independent experiments run in triplicate.

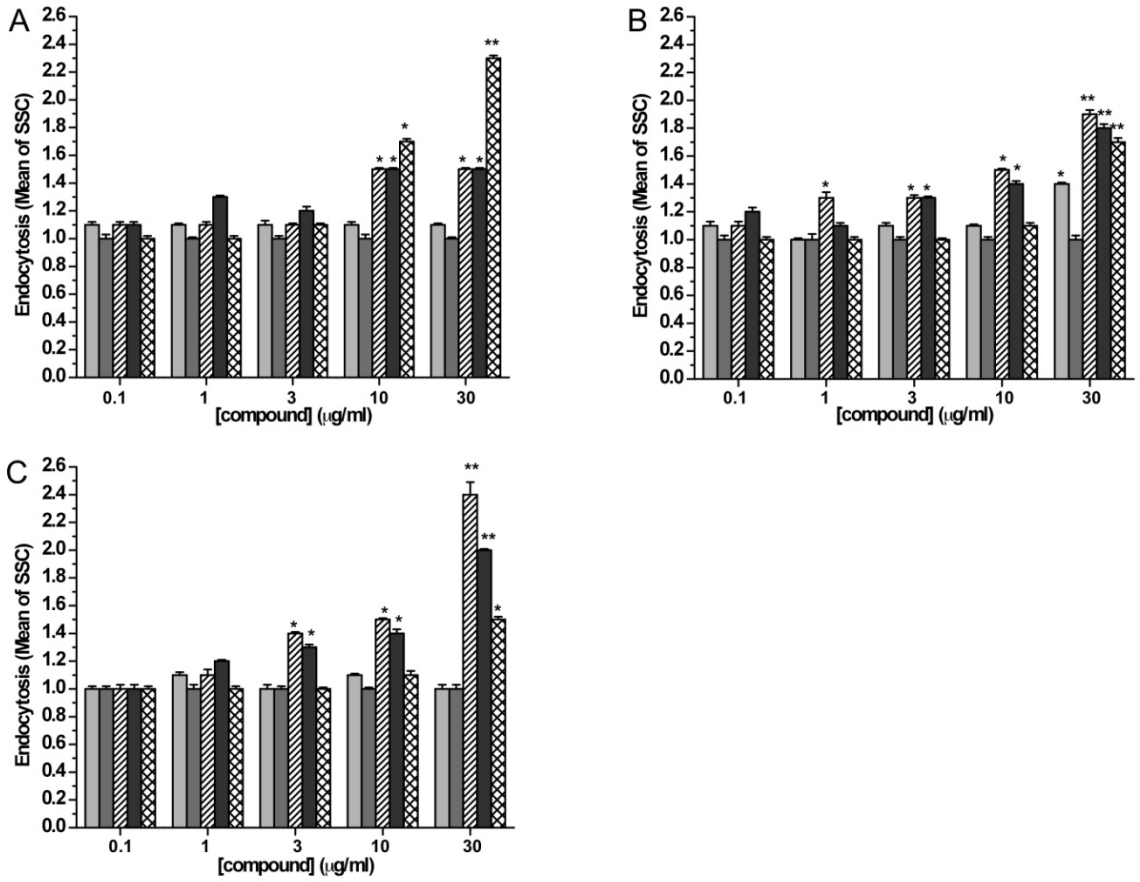

Figure S8: Concentration-dependence of **2**, polyethylene glycol-coated MNPs (**PEMNPs**), citrate-coated MNPs (**CMNPs**), and glycosyl MNPs (**2MNPs** and **GlcMNPs**) uptake. RAW 264.7 cells were treated with increasing concentrations (0.1-30 μg/ml) of **2** (light grey bars), **PEMNPs** (grey bars), **CMNPs** (hatched bars), **GMNPs** (dark grey bars) or **GlcMNPs** (cross-hatched bars)**,** for 24h (A), 48h (B) and 72 h (C). In each sample, the compound uptake was quantified by FACS. The data represent mean ± SEM of at least three independent experiments. *$p \leq 0.05$; **$p \leq 0.01$ vs. controls (untreated cells).

Table S1. PCR primers and protocols used in this study

Template	*Primers*	*Size (bp)*	*Denaturation*	*Annealing*	*Extension*	*Cycles*
mTNFα	forward 5'- CCTGTAGCCCACGTCGTACG-3'	363	94˚C for 30 s	56˚C for 30 s	72˚C for 45 s	30
NM_013693[a)]	reverse 5'- TTGACCTCAGCGCTGAGTTG-3'					
mβ-actin	forward 5'-TGTGATGGTGGGAATGGGTCAG-3'	514	94˚C for 1 min	65˚C for 1 min	72˚C for 1 min	26
NM_007393[a)]	reverse 5'-TTTGATGTCACGCACGATTTCC-3'					

[a)] Accession number NCBI sequence database (GenBank)

References

[S1] Schmidt, R. R.; Jung K.-H. in Preparative Carbohydrate Chemistry Ed. S.Hanessian Marcel Dekker, New York;**1997**, p.283.

[S2] Arcangeli, A.; Toma, L.; Contiero, L.; Crociani, O.; Legnani, L.; Lunghi, C.; Nesti, E.; Moneti, G.; Richichi, B.; Nativi C. Stable GM3 lactone mimetic raises antibodies specific for the antigens expressed on melanoma cells *Bioconjugate Chem.* **2010**, *21*, 1432-1438.

[S3]Wu, X.; Ling, C.-C.; Bundle, D. A new homobi-functionalp-nitro phenyl ester coupling reagent for the preparation of neoglycoproteins. Org. Lett. **2004**, *6*, 4407-4410.